ELSEVIER

Journal of Power Sources 104 (2002) 148–153

JOURNAL OF POWER SOURCES

www.elsevier.com/locate/jpowsour

Short communication

Camphor-based carbon nanotubes as an anode in lithium secondary batteries

M. Sharon[a,*], W.K. Hsu[b], H.W. Kroto[b], D.R.M. Walton[b], A. Kawahara[c], T. Ishihara[c], Y. Takita[c]

[a]*Chemistry Department, Indian Institute of Technology, Bombay 400076, India*
[b]*School of Chemistry, Physics and Environmental Science, University of Sussex, Brighton, BN1 9Q, UK*
[c]*Department of Applied Chemistry, Faculty of Engineering, Oita University, Dannoharu 700, Oita 870-1192, Japan*

Received 21 May 2001; received in revised form 4 June 2001; accepted 26 July 2001

Abstract

Camphor vapour is pyrolysed in the presence of Fe, Ni and Co powder under a dinitrogen atmosphere at different temperatures (750–1050 °C). While Fe and Ni catalyse the formation of carbon nanotubes (CNs), Co facilitates carbon nanobead growth. The CNs, obtained using a Fe catalyst at 950 °C, are utilised as the anode in Li secondary batteries. The capacity of the batteries constructed in this way is as good as those prepared by graphitic carbon formed in the arc process.

Keywords: Camphor; Carbon nanotube catalyst; Lithium battery carbon; Lithium intercalation camphoric carbon

1. Introduction

Lithium secondary batteries are the only commercially available types capable of producing greater than 3 V per cell. Optimisation of their performance is therefore desirable, especially with respect to the anode capacity. Lithium metal anodes, used in conjunction with an organic electrolyte, result in non-uniform formation of a passive film on the anode surface [1–3] which causes dendritic growth of lithium metal. This problem is tackled by utilising the electrochemical intercalation of lithium in carbon [4], which generates a considerable negative potential close to that of lithium, but which is less reactive and easily reversible. The structural characteristics of carbon are believed to be the major element that controls the performance of Li-ion batteries. Thus the intercalation of Li-ion with carbon depends upon factors such as the preparative history, carbon precursor, etc. Till date, studies have focused mainly on Li-intercalation into graphitic materials [5]. The stoichiometric limit, Li-intercalation (C_6Li), of 372 mAh g^{-1} has motivated the development of higher capacity anodes. Recently, attention has been drawn to disordered carbon materials [6], which may store Li via a mechanism which is completely different from that associated with graphite. It is believed that small crystallite size and random crystallite orientation may increase the number of Li ions per carbon atom. Carbon nanotubes (CNs), made by arc discharge, are highly graphitised due to the 3000–4000 °C arc temperature, i.e. annealing occurs. Nevertheless, CNs prepared by a templating method are very defective and exhibit a large Li-ion intercalation capacity, viz, 350–780 mAh g^{-1} [7–12]. The plateau potentials exhibited by the charge-discharge curves for these non-graphitic carbons are remote from 0 V and the potentials gradually decrease as the intercalated-Li content increases [13]. Ishihara et al. [11] studied the effect of the size of CNs in relation to capacity performance of Li-ion batteries. It was found that the maximum reversible capacity was obtained with a graphite tube of 40 m^2 g^{-1} surface area. Sharon and co-workers [14,15] studied the intercalation of lithium with camphor-based carbon nanobeads and found the cell to be stable for 10–20 days. The reversible Li-ion intercalation capacity was found to be 0.45–0.61 V. In this paper, we describe the influence of camphor-based CNs on the performance of Li-ion batteries.

2. Experimental

2.1. Preparation of carbon nanotubes from camphor

The pyrolysis apparatus consisted of a two-stage digitally-controlled furnace, as described previously [16]. 200 mg of

* Corresponding author. Tel.: +91-22-578-2545/3124; fax: +91-22-576-7152.
E-mail address: sharon@chem.iitb.ac.in (M. Sharon).

0378-7753/02/$ – see front matter
PII: S0378-7753(01)00872-2

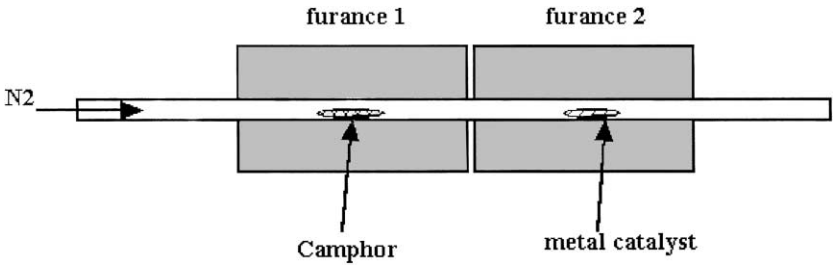

Fig. 1. Apparatus for camphor pyrolysis.

camphor (Camphor and Allied Products Ltd., India) was placed in one furnace (#1) and metal catalysts (Fe, Ni and Co, 50 mg, 325 mesh, Aldrich, UK) were placed in a second furnace (#2), see Fig. 1. A flow of nitrogen (50–100 cm^3 min^{-1}) was introduced. The pyrolysis temperature was set at 750, 850, 950 and 1050 °C, respectively, and the temperature of furnace #1, was gradually increased (20 °C min^{-1}) to 400 °C in order to vapourise completely the camphor, which was transferred to furnace #2 by N_2. After cooling, the materials collected from furnace #2 were analysed by transmission electron microscopy (TEM) and used as anode material in the lithium secondary battery.

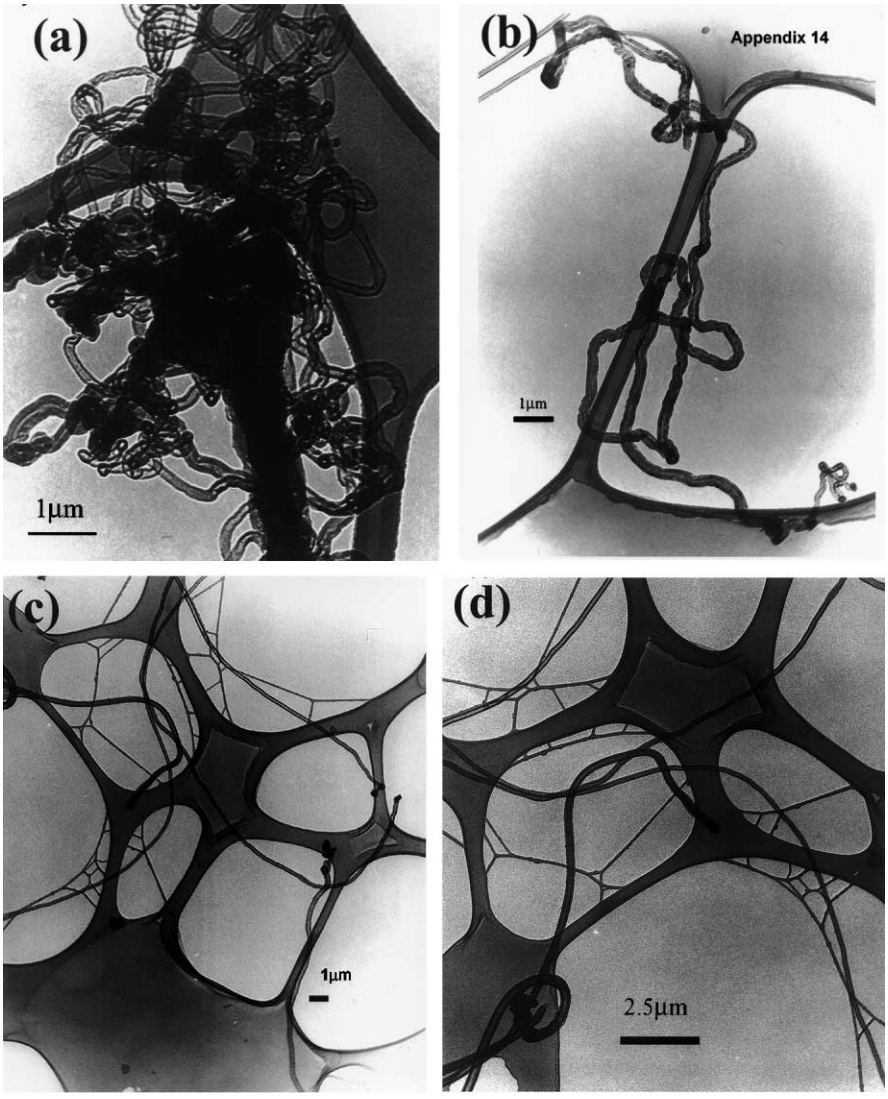

Fig. 2. TEM images of Fe-camphor-CNs at (a) 750 °C, (b) 850 °C, (c) 950 °C and (d) 1050 °C in presence of N_2 flow.

2.2. Secondary electrode in lithium battery

Each carbon sample was mixed with ethylene-propylene-dimethyl-monomer (EPDM) in cyclohexane and then pressed into a stainless-steel grid on the stainless-steel plate as an anode. A constant dc current (0.4 mA cm^{-2}) was applied across the anode and a Li-metal counter electrode in order to record the Li-intercalation capacity of the anode. Ethylene carbonate (EC):dimenthyl carbonate (DMC) (1:20 solution), dissolved in $LiPF_6$ (1 wt.%), was used as an electrolyte. The charge–discharge characteristics were measured between 0 and 1.5 V.

3. Results and discussion

3.1. Transmission electron microscopy

The results of TEM observations are summarised in Table 1. TEM images of samples, produced by pyrolysing camphor at 750, 850, 950 and 1050 °C are shown, respectively, in Fig. 2(a)–(d) for the Fe-catalyst, in Fig. 3(a)–(d) for Ni and in Fig. 4(a)–(d) for Co.

With the Fe catalyst, the yield of CNs decreases as the pyrolysis temperature increases (750–1050 °C, Fig. 2(a)–(d)). The degree of graphitisation in CNs increases, however, with increasing pyrolysis temperature (950–1050 °C, Fig. 2(c) and (d)). In Ni-catalysed pyrolysis, CNs were produced at the low temperature (i.e. 750 °C, Fig. 3(a)), together with large Ni-particles. In contrast to Fe, the Ni-catalysed CNs are not well-defined, in particular the degree of graphitisation decreases at relatively high temperature (850 °C, Fig. 3(b)). Small amounts of Ni-filled tube-like materials, however, were produced (Fig. 3(b) and (c)). The CNs and Ni-filled tube-like materials were completely absent when the temperature was increased to 1050 °C; only large Ni-encapsulated carbon particles were generated (Fig. 3(d)). The Fe and Ni exhibit opposite effects at these operating temperatures. The yield of CNs in Fe-camphor pyrolysis at 950–1050 °C is similar to that of Ni-camphor pyrolysis at 750 °C (∼40%).

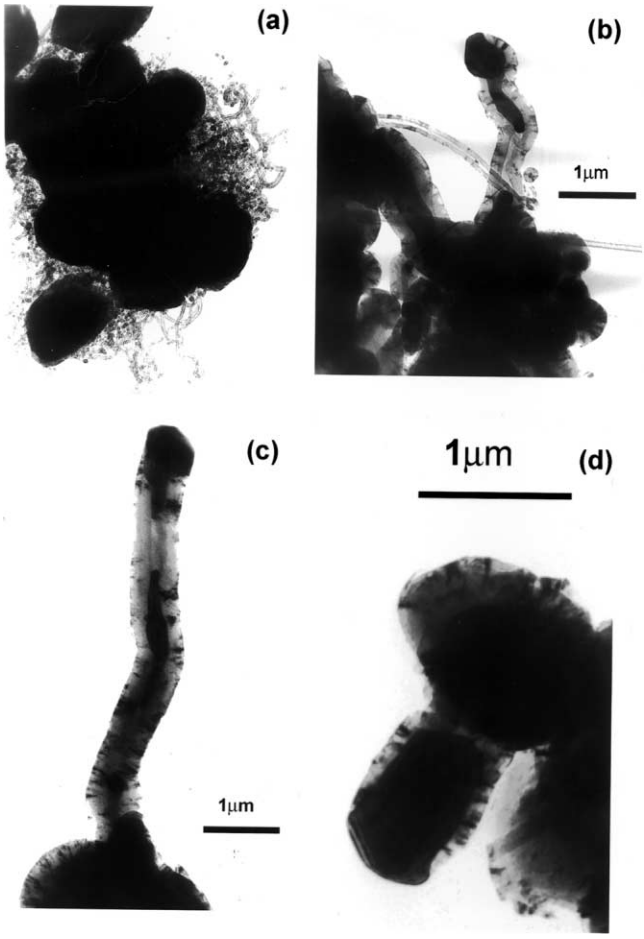

Fig. 3. TEM images of Ni-camphor-CNs at (a) 750 °C, (b) 850 °C, (c) 950 °C and (d) 1050 °C in presence of N_2 flow.

With the Co-catalyst at 750–1050 °C, carbon nanobeads (1–1.5 μm, in diameter), possibly containing Co, were produced in bulk (Fig. 4(a)–(d)); CNs were absent. At 750–850 °C, carbon particles encapsulated with Co metal were

Table 1
Summary of dimensions of CNs formed with different catalyst at different temperatures[a]

Catalyst	750 °C	850 °C	950 °C	1050 °C	Remarks
Fe					
d_1 (nm)	250	300	500	500	No nanobeads formed
d_2 (nm)	50	60	130	125	
L (μm)	12	18	18	20	
Ni					
d_1 (nm)	30	180	600	No nanotube	No nanobeads formed
d_2 (nm)	9	160	230		
L (μm)	Very small	Very small	Very small		
Co					
d_1 (nm)	750–850	950–1050	950–1050	No nanobead or nanotube	Only nanobeads formed
d_2 (nm)	30	–	–		
L (μm)	Spherical	Spherical	Spherical		

[a] d_1 (nm) is the external diameter, d_2 (nm) the thickness of nanotube and L (μm) the length of nanotube.

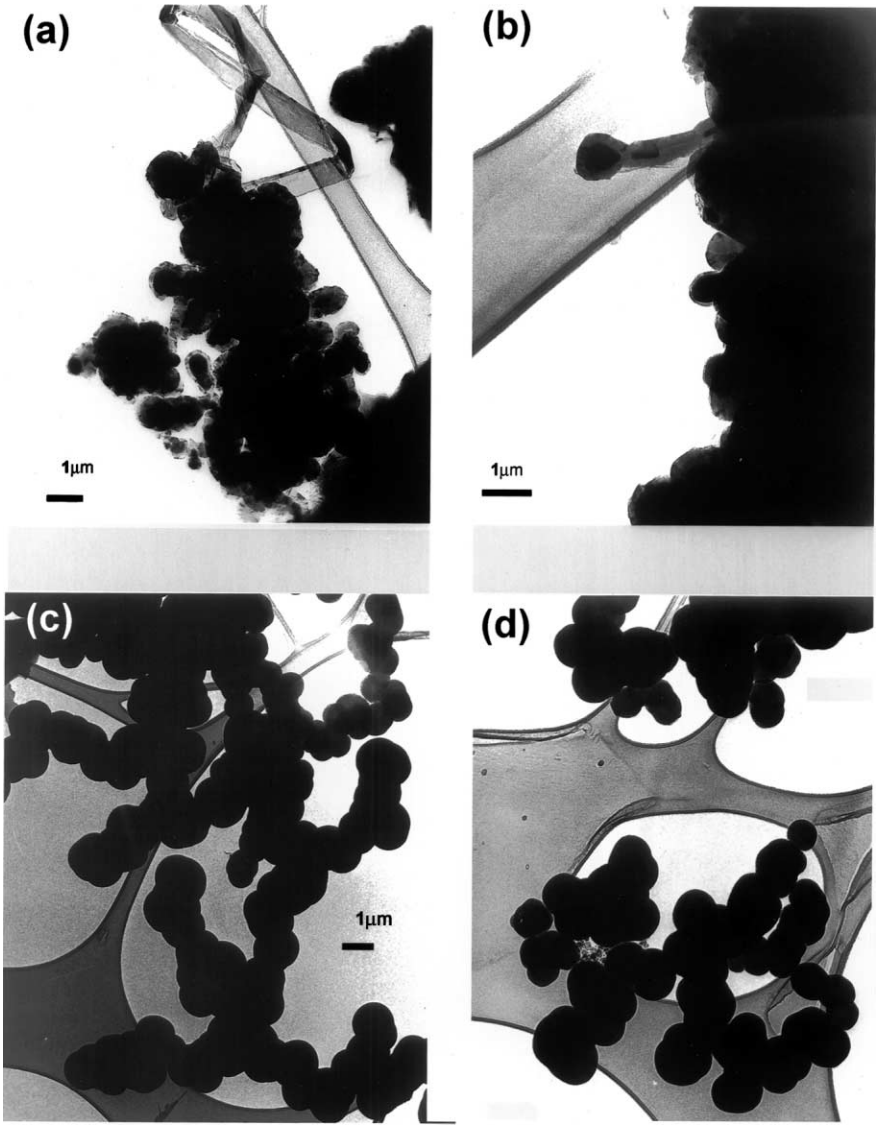

Fig. 4. TEM images Co-camphor-CNs at (a) 750 °C, (b) 850 °C, (c) 950 °C and (d) 1050 °C in presence of N_2 flow.

produced (Fig. 4(a) and (b)). The structure of the carbon nanobeads is similar to that given in a previous report [16].

3.2. Lithium battery

In order to compare camphor-based CNs (referred as sample 1), obtained using Fe-catalyst at 950 °C, arc-made CNs (referred as sample 2) and boron-doped CNs (referred as sample 3, Fig. 5), the samples [17] were used as anodes in Li-intercalation measurements. Charge–discharge profiles, as a function of potential versus capacity and capacity versus charge–discharge time, were recorded. The charge–discharge curves for Li-intercalation capacity are presented in Figs. 6–8. It is clear that camphor-CNs are capable of intercalating Li. Sample 2 (Fig. 6) and 3 (Fig. 7) exhibits an irreversibility and gradual decrease in potential; no significant stage was observed on the charge–discharge curves. The presence of irreversible capacity in samples 2 and 3 might be due to the large amorphous carbon content. Sample 1 (Fig. 8) exhibits a much larger irreversible capacity (180 mAh g^{-1}) for Li-intercalation. In addition, two stages for Li interaction are observed at 0.2 and 0.1 V. This result is typical for Li-ion intercalation performance on graphite. It has been reported [18] that three stages of lithium intercalation occur in graphitic carbon. Accordingly, sample 1 contains a large portion of graphitic material and displays a promising anode performance for Li-ion rechargeable batteries. This outcome is superior to that of CH_4-pyrolysed grown CNs, which exhibit small initial and reversible Li-intercalation capacities [10,11].

The Li-intercalation capacity of sample 1, as a function of cycle number, is given in Fig. 9. It is clear that during the first cycle, a large irreversible capacity is present. After the second cycle, however, almost 100% coulomb efficiency is obtained. After 5 cycles, the irreversible capacity of 175 mAh g^{-1} is sustained. This indicates that the cycle

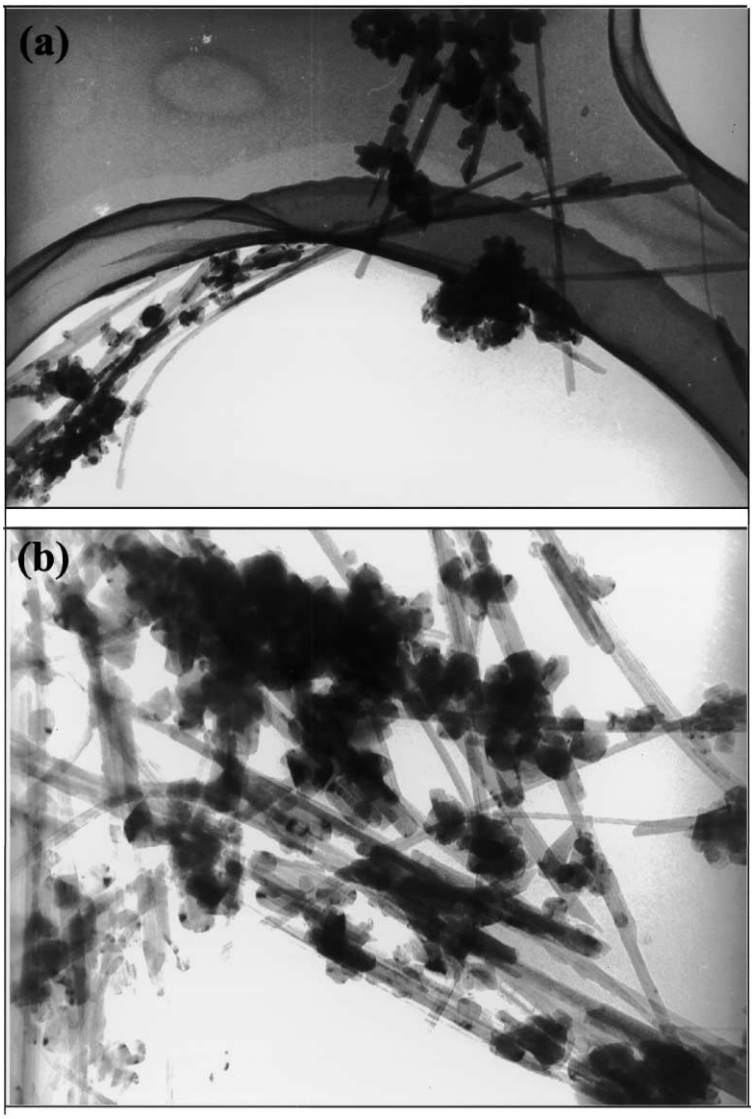

Fig. 5. (a) TEM image of arc-made CNs, (b) TEM image of arc-made boron doped CNs.

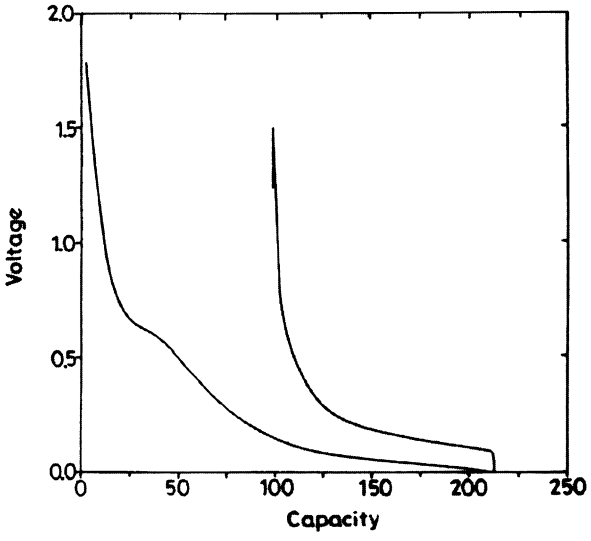

Fig. 6. Charge–discharge curve of arc-made CNs (sample 2). Charge capacity is 213 mAh g^{-1} and discharge capacity is 114 mAh g^{-1}.

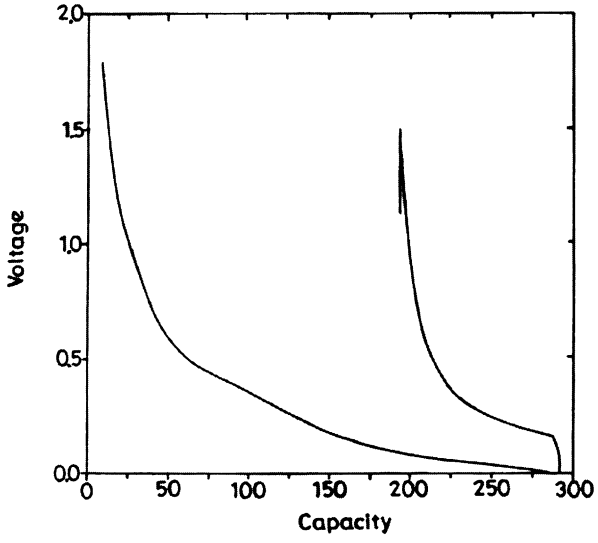

Fig. 7. Charge–discharge curve of arc-made boron doped CNs (sample 3). Charging capacity is 292 mAh g^{-1} and discharge capacity is 98 mAh g^{-1}.

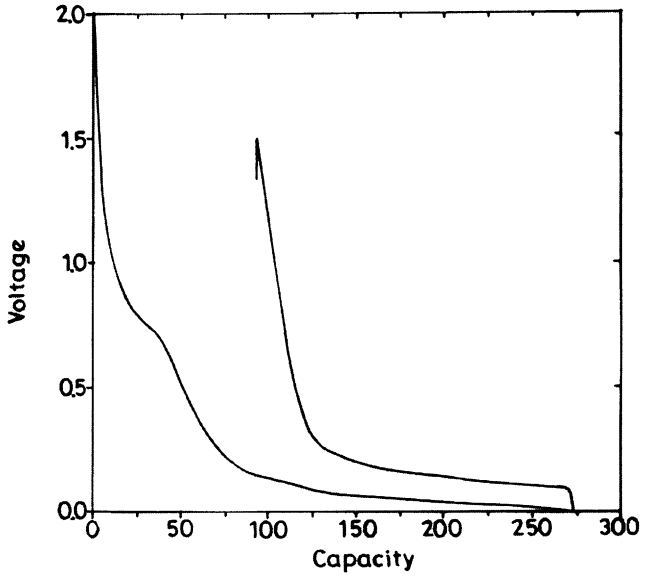

Fig. 8. Charge–discharge curve of CNs (sample 1), obtained by pyrolysing camphor at 950 °C (Fig. 2(c)) using Fe as catalyst. Charging capacity is 273 mAh g^{-1} and discharge capacity is 180 mAh g^{-1}.

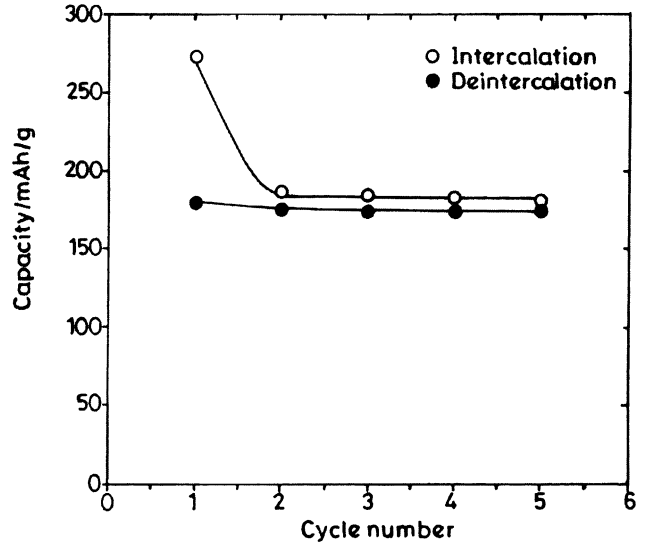

Fig. 9. Li-intercalation capacity as function of cycle number for arc-made boron doped CNs (sample 1, Fig. 2(c)).

stability of camphor-based CNs (sample 1) in the Li-intercalation process is relatively high, as compared with that of bulk graphite. The Li-interaction content can be increased at the anode, if Li^+ is able to diffuse into the interior of the CNs.

4. Conclusions

Camphor-based CNs exhibit relatively high irreversibility in charging–recharging profiles and good cycle stability, as compared with arc-made CNs and boron-doped CNs.

References

[1] E. Peled, J. Electrochem. Soc. 126 (1979) 2047.
[2] V.R. Koch, J.L. Goldman, C.J. Mattos, M. Mulvaney, J. Electrochem. Soc. 129 (1982) 1.
[3] T. Hirai, I. Yoshimatsu, J. Yamaki, J. Electrochem. Soc. 141 (1994) 2300.
[4] A. Herold, Bull. Soc. Chim. France 187 (1955) 999.
[5] C. Wang, I. Kakwan, A.J. Appleby, F.E. Little, J. Electroanal. Chem. 489 (2000) 55.
[6] S. Wang, H. Matsui, H. Tamamura, Y. Matsumura, Phys. Rev. B 58 (1998) 8163.
[7] G. Che, B.B. Lakshmi, E.R. Fischer, C.R. Martin, Nature 398 (1998) 346.
[8] G.T. Wu, C.S. Wang, X.B. Zhang, H.S. Yang, Z.F. Qi, P.M. He, W.Z. Li, J. Electrochem. Soc. 146 (1999) 1696.
[9] A.S. Claye, J.E. Fisher, C.B. Huffman, A.G. Rinzler, R.E. Smalley, J. Electrochem. Soc. 147 (2000) 2845.
[10] G. Maurin, C. Bousquet, F. Henn, P. Bernier, R. Almairac, B. Simon, Chem. Phys. Lett. 312 (1998) 14.
[11] T. Ishihara, A. Fukunaga, R. Akiyoshi, M. Yoshio, Y. Takita, Electrochem. 68 (2000) 38.
[12] F. Beguin, K. Metenier, R. Pellenq, S. Bonnamy, E. Frackowiak, Mol. Cryst. Liq. Cryst. 340 (2000) 547.
[13] M. Hara, A. Satoh, N. Tamaki, T. Ohsaki, J. Phys. Chem. 99 (1995) 16338.
[14] M. Sharon, M. Kumar, P.D. Kichambre, N.R. Avery, K.J. Black, Mol. Cryst. Liq. Cryst. 340 (2000) 523.
[15] M. Kumar, P.D. Kichambre, M. Sharon, N.R. Avery, K.J. Black, Mat. Chem. Phys. 66 (2000) 83.
[16] M. Sharon, K. Mukhopadhyay, K. Yase, S. Iijima, Y. Ando, X. Zhao, Carbon 36 (1998) 507.
[17] W.K. Hsu, S.Y. Chu, E. Munoz-Picone, J.L. Boldu, S. Firth, P. Franchis, B.P. Roberts, A. Schilder, H. Terrones, N. Grobert, Y.Q. Jhu, M. Terrones, M.E. Mc Henry, H.W. Kroto, D.R.M. Walton, Chem. Phys. Lett. 323 (2000) 572.
[18] M. Winter, P. Novak, A. Monnier, J. Electrochem. Soc. 145 (1998) 428.